

# Entropic Lattice Boltzmann Method for Large Scale Turbulence Simulation

By I. V. KARLIN<sup>1</sup> † S. ANSUMALI<sup>1</sup> E. DE ANGELIS<sup>1</sup> ‡  
 H. C. ÖTTINGER<sup>1</sup>  
 AND  
 S. SUCCI<sup>2</sup>

<sup>1</sup> ETH-Zürich, Department of Materials, Institute of Polymers, ETH-Zentrum, Sonneggstr. 3, ML J 19, CH-8092 Zürich, Switzerland

<sup>2</sup>Istituto Applicazioni Calcolo, CNR, viale Policnico 137, 00161 Roma, Italy

(Received 30th May 2003)

Recently, a minimal kinetic model for fluid flow, known as entropic lattice Boltzmann method, has been proposed for the simulation of isothermal hydrodynamic flows. At variance with previous Lattice Boltzmann methods, the entropic version permits to describe the non-linear dynamics of short scales in a controlled and stable way. In this paper, we provide the first numerical evidence that the entropic lattice Boltzmann scheme provides a quantitatively correct description of the large-scale structures of two-dimensional turbulence, free of numerical instabilities. This indicates that the entropic lattice Boltzmann method might provide a starting basis for the formulation of a new class of turbulence models based on genuinely kinetic principles.

## 1. Introduction

{ } The dynamics of fully developed turbulent flows is characterized by the simultaneous non-linear interaction of a large number of degrees of freedom, far too many for analytical treatment and also for the processing capabilities of even most powerful computers. Since most turbulent flows of practical relevance cannot be simulated *ab initio*, they must be modeled. The goal of such a modeling is to predict the effects of unresolved scales of motion, those that cannot be represented within the computer simulation, on the resolved ones. Mathematically, these effects are represented by the divergence of the Reynolds stress tensor,  $\mathbf{\Gamma} = \langle \mathbf{u}'\mathbf{u}' \rangle$ , where  $\mathbf{u}'$  denotes the short-scale component of fluid motion, and the pointed bracket stands for ensemble averaging.

A popular class of models is based on the notion of ‘eddy-viscosity’, according to which the effects of short scales can be incorporated within an effective viscosity  $\nu_e = \nu + \nu_t$  acting upon the large scales. Here  $\nu$  is the bare, ‘molecular’ viscosity, whereas  $\nu_t$  denotes the turbulent viscosity. The effective viscosity  $\nu_e$  is then expressed as a function(al) of resolved fields. The simplest option consists of choosing a suitable algebraic relation  $\nu_t = \nu_t(S)$ , where  $S$  is the magnitude of the shear tensor  $\mathbf{S} = \nabla\mathbf{U} + \nabla(\mathbf{U})^T$ ,  $\mathbf{U}$  denoting the resolved flow field. The simplest eddy-viscosity models express the Reynolds stress tensor in an algebraic form:  $\mathbf{\Gamma} = \nu_e(\mathbf{S})\mathbf{S}$ . This formulation has the significant advantage of leaving the form of the Navier-Stokes equation for the large eddies intact, with

† Corresponding author. E-mail: ikarlin@mat.ethz.ch

‡ permanent address: Dip. di Meccanica e Aeronautica, Università di Roma “La Sapienza”, Via Eudossiana, 18 00184 Roma, Italy

an effective viscosity  $\nu_e$  replacing the molecular viscosity  $\nu$ . However, such an algebraic representation often fails to reproduce strongly off-equilibrium turbulent effects, such as those occurring in the vicinity of solid walls. A better account of these phenomena is obtained by linking  $\nu_e$  to the actual content of turbulent kinetic energy  $k = \langle \mathbf{u}'^2/2 \rangle$  and energy dissipation rate  $\epsilon = dk/dt$ , via  $\nu_e \sim k^2/\epsilon$ . Even so, important phenomena such as turbulent gusts triggered by local instabilities (corresponding to negative effective viscosity) cannot be captured (Kraichnan 1976) because  $\nu_e$  is bound to be positive definite. Modern formulations which allow for negative viscosities and corresponding backscatter effects in  $k$ -space have indeed been developed in the last two decades (Lesieur and Metais 1996). However, to the best of our knowledge, none of these models has gained universal consensus to date.

All eddy-viscosity models rely on the analogy between the turbulent transport and the molecular transport. Within this analogy, the small-scale eddies play the role of the molecules, while the smallest coherence length,  $l_k$ , known as Kolmogorov length, plays the role of the mean-free path. It is then natural to define a ‘turbulent Knudsen number’ for an eddy of size  $l$  as

$$Kn_t(l) = \frac{l_k}{l}$$

It is then understood that small-scale eddies of size close to  $l_k$  are in local equilibrium with eddies of size  $l$ , so long as these two scales are well separated, i.e.  $Kn_t(l) \ll 1$ .

A major problem with this analogy is that turbulence features a *continuum* spectrum of excitations, so that the above scale-separation argument simply does not hold. In particular, from the above definition of turbulent Knudsen number, it is clear that the local equilibrium assumption becomes less and less tenable as  $l \rightarrow l_k$ . This lack of scale separation is a fundamental problem which lies the heart of all failures to develop a consistent theory of fully developed turbulence.

From the computational point of view, the Kolmogorov length is replaced by the grid spacing  $\delta \gg l_k$ , indicating that the dynamics of the smallest resolved scales faces a situation similar to finite-Knudsen flows at  $Kn \sim 1$ .

It has been recently pointed out that the kinetic representation of hydrodynamics provides a natural generalization of the notion of eddy-viscosity to such non-equilibrium high- $Kn_t$  regimes (Chen *et al.* 1999, 2003). The key point is that solutions of the kinetic equation apply at *all* orders of the Knudsen number, so that *any* kinetic model ensuring correct hydrodynamic behaviour would handle the dynamics of small eddies at  $Kn_t \sim 1$  in a way which goes beyond the eddy-viscosity representation.

The practical problem with kinetic theory, however, is the enormous increase of degrees of freedom associated with the (true) Boltzmann equation. Thus, in order to apply the aforementioned kinetic approach to fluid turbulence, drastically simplified versions of the Boltzmann equation need to be developed. The lattice Boltzmann method (hereafter LBM) (Succi 2001; Benzi *et al.* 1992), is a good candidate for such a task. Indeed, the method has been applied to a large variety of fluid flows, including turbulent ones (Benzi and Succi 1990; Martinez *et al.* 1994). However, the standard lattice Boltzmann method meets with severe difficulties in handling the dynamics of near-grid scales with  $l \sim \delta$ . In particular, owing to the lack of a H-theorem, these scales often exhibit disruptive non-linear instabilities.

Recently, a new approach to stabilize the kinetic scheme based on thermodynamic considerations was developed (Karlin *et al.* 1999; Ansumali and Karlin 2002a,b,c; Boghosian *et al.* 2001). The modified method known as ‘‘entropic Lattice Boltzmann method’’ might add a further boost towards the formulation of a kinetic model of fluid turbulence. In par-

ticular, its non-linear stability, and the ensuing positivity of the distribution function, automatically enforces an important realizability constraint which is missing in standard Lattice Boltzmann representations. More specifically, this model provides a local, adaptive, regulator of the relaxation time, which can be regarded to all effects and purposes as a turbulence model inspired by genuinely kinetic requirements. In this paper, we present a set of numerical experiments which are intended to test this conjecture in a semi-quantitative sense.

The work is organized as follows: first, a description of the LBM and its entropic version is introduced (Sec. 2). Then, simulations of two dimensional decaying turbulence are presented for the fully resolved as well as unresolved case (Sec. 3). For validation purposes, results are compared with spectral simulation of the Navier–Stokes equations in the fully resolved case.

## 2. Lattice kinetic theory

In the last decade, it has become apparent that minimal versions of the Boltzmann kinetic equation provide a fairly efficient alternative to the discretisation of the Navier–Stokes equations for the simulation of a variety of complex flows, including turbulent ones (Succi 2001). In its simplest instance, this minimal kinetic equation takes the following form:

$$\partial_t f_i + \mathbf{c}_i \cdot \partial_{\mathbf{x}} f_i = -\tau^{-1} (f_i - f_i^{eq}), \quad (2.1)$$

where  $f_i \equiv f(x, \mathbf{c}_i, t)$  denotes the probability of finding a particle at position  $x$  and time  $t$ , moving along the discrete direction  $\mathbf{c}_i$ . The right-hand-side of this equation represents collisional relaxation to a local equilibrium on a time scale  $\tau$ . The discrete velocities must be chosen in such a way as to ensure sufficient symmetry to recover the basic mass, momentum and momentum-flux conservations, so that the Navier–Stokes equations are recovered as the large-scale limit of the discrete kinetic equation. For this purpose, many options have become available over the years. The major appeal of the kinetic approach is its remarkable simplicity, which translates into a corresponding computational efficiency. A distinctive mark of this simplicity is the fact that, *i*) the streaming operator is linear and proceeds along a set of constant directions, *ii*) the non-linearity is entirely due to the local equilibrium, which is fully local in configuration space. This is in vivid contrast to the Navier–Stokes representation in which both non-locality and non-linearity are condensed into a single term, namely the convective operator  $\mathbf{u} \cdot \partial_{\mathbf{x}} \mathbf{u}$ . Typically, the local equilibrium is chosen in the form of a quadratic polynomial in the fluid speed :

$$f_i^{eq} = \rho W_i \left[ 1 + k_1 \mathbf{c}_i \cdot \mathbf{u} + k_2 (\mathbf{c}_i \cdot \mathbf{u})^2 + k_3 (\mathbf{c}_i \mathbf{c}_i) : (\mathbf{u} \mathbf{u}) \right], \quad (2.2)$$

where,  $W_i, k_1, k_2$ , and  $k_3$  are lattice dependent constants depending on the lattice sound speed  $c_s$  (a constant for the present case of athermal flows). The advantage of this approach is that local equilibria can be readily constructed after particles have gone through the streaming phase. Subsequent irreversible relaxation to this local equilibrium provides viscous behavior, with a kinematic viscosity of the order of  $\nu \sim c_s^2 \tau$ . The simplicity of this scheme is hard to beat. However, the fact that local equilibria are prescribed at the outset and do not result from a self-consistent relaxation dynamics in kinetic space, implies that compliance with the second law of thermodynamics, the H-theorem in kinetic language, is generally lost (Succi *et al.* 2002). The result is that, whenever large gradients develop on the lattice scale, as it is the case for fully developed turbulence, standard LBE schemes are subject to numerical instabilities. This provides a strong mo-

tivation to develop a new class of lattice Boltzmann schemes, capable of accommodating the  $H$  theorem. A particularly interesting option has recently emerged in the form of the so-called entropic Lattice Boltzmann method (ELBM) (Ansumali and Karlin 2002c). In remainder of this section we will describe entropic model.

The basic strategy of the entropic Lattice Boltzmann method is to write the dynamics in terms of a properly chosen  $H$  function (Karlin *et al.* 1999; Ansumali and Karlin 2002c). For isothermal hydrodynamics, the discrete  $H$  function is found to be in Boltzmann-form:

$$H_{\{W_i, \mathbf{c}_i\}} = \sum_{i=1}^{b^D} f_i \ln \left( \frac{f_i}{W_i} \right), \quad (2.3)$$

where  $b^D$  is the number of discrete velocities in  $D$ -dimensions. The discrete velocities are tensor products of the discrete velocities in one dimension and the weights are constructed by multiplying weights associated with each direction. The minimal set of discrete velocities needed to reconstruct the Navier-Stokes equations are related to zeroes of third-order Hermite polynomials in  $c_i$  and for  $D = 1$ , the three discrete velocities are  $c_i = c\{-1, 0, 1\}$ , whereas the corresponding weights are  $w = \{\frac{1}{6}, \frac{2}{3}, \frac{1}{6}\}$  (Shan and He 1998). The discrete-velocity local equilibrium is the minimizer of the corresponding entropy function under the constraint of local conservation laws:  $\sum_{i=1}^{b^D} f_i^{\text{eq}} \{1, \mathbf{c}_i\} = \{\rho, \rho \mathbf{u}\}$ . The explicit solution for the  $f_i^{\text{eq}}$  is

$$f_i^{\text{eq}} = \rho W_i \prod_{j=1}^D \left( 2 - \sqrt{1 + 3u_j^2} \right) \left( \frac{2u_j + \sqrt{1 + 3u_j^2}}{1 - u_j} \right)^{c_{ij}/c}, \quad (2.4)$$

with  $j$  being the index for spatial directions. Further, a notion of the bare collision  $\mathbf{\Delta}$ , defined as the collision term stripped of its relaxation parameters is introduced. In the case of BGK model  $\mathbf{\Delta} = \mathbf{f}_{\text{eq}} - \mathbf{f}$ , namely the bare departure from local equilibrium. The time stepping in this method is performed through an over-relaxation collisional process and linear convection through a sequence of steps in which the  $H$  function is bound not to decrease. The monotonicity constraint on the  $H$  function is imposed through the following geometric procedure: In the first step, populations are changed in the direction of the bare collision in such a way that the  $H$  function remains constant. In the second step, dissipation is introduced and the magnitude of the  $H$  function decreases. Thus,

$$f_i(\mathbf{x}, \delta t) = f_i(\mathbf{x} - \mathbf{c}_i \delta t, 0) + \alpha \beta \left[ f_i^{\text{eq}}(\mathbf{x} - \mathbf{c}_i \delta t, 0) - \mathbf{f}(\mathbf{x} - \mathbf{c}_i \delta t, 0) \right] \quad (2.5)$$

where  $\beta$  is the discrete form of the relaxation frequency related to  $\tau^{-1}$  and the parameter  $\alpha$  is defined by the condition:

$$H(\mathbf{f}) = H(\mathbf{f} + \alpha \mathbf{\Delta}), \quad (2.6)$$

and close to the local equilibrium  $\alpha$  is equal to 2 (Ansumali and Karlin 2002a). The scheme is illustrated graphically in figure 1. As shown in figure 1, in order to find the desired point  $\mathbf{f}(\beta)$ , we first find the point  $\mathbf{f}^*$  on the curve  $L$  of constant  $H$  function. This way of enforcing the  $H$  theorem ensures non-linear stability. An algorithm to implement Eq. (2.6) has been presented by Ansumali and Karlin (2002a). The local adjustments of the relaxation time (via the parameter  $\alpha$ ), as dictated by compliance with the H-theorem, guarantee positivity of the distribution function also for the case of discrete steps, thereby ensuring non-linear stability of the numerical scheme.

A comment on the relation between non-linear stability and built-in subgrid modelling

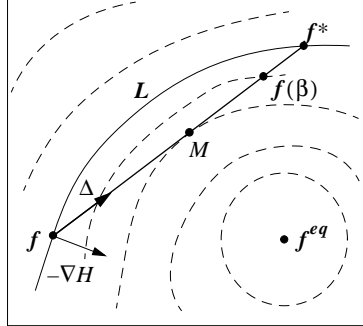


FIGURE 1. Stabilization procedure. Curves represent entropy levels, surrounding the local equilibrium  $\mathbf{f}^{eq}$ . The solid curve  $L$  is the entropy level with the value  $H(\mathbf{f}) = H(\mathbf{f}^*)$ , where  $\mathbf{f}$  is the initial, and  $\mathbf{f}^*$  is the auxiliary population. The vector  $\Delta$  represents the collision integral, the sharp angle between  $\Delta$  and the vector  $-\nabla H$  reflects the entropy production inequality. The point  $\mathbf{f}^*$  is the solution to Eq. (2.6). The result of the collision update is represented by point  $\mathbf{f}(\beta)$ . The choice of  $\beta$  shown corresponds to the ‘over-relaxation’:  $H(\mathbf{f}(\beta)) < H(\mathbf{f})$  but  $H(\mathbf{f}(\beta)) > H(\mathbf{M})$ . The particular case of the BGK collision (not shown) would be represented by a vector  $\Delta_{BGK}$ , pointing from  $\mathbf{f}$  towards  $\mathbf{f}^{eq}$ , in which case  $\mathbf{M} = \mathbf{f}^{eq}$ .

is in order. As is well known, in a turbulent flow energy (enstrophy in two-dimensional set up) cascades from large to small scales. While physically the cascade picture is terminated by dissipation at the Kolmogorov length  $l_k$ , in an underresolved simulation, the cascade needs to be truncated at the grid spacing  $\delta > l_k$ . As the entropy of the ELBM (“grid entropy”) accounts for the net effect of *all* degrees of freedom that are not resolved in the simulation (including the physical entropy), it provides the natural key to implementing artificial dissipation on the grid scale. According to the H theorem, the cascade is terminated on the grid scale in such a way that the subgrid scales cannot “fire back” at scales larger than  $\delta$ . Consequently, the grid entropy of the ELBM allows us to decouple all subgrid effects from the cascade in a most natural way. This is exactly the goal traditionally approached with the concept of eddy-viscosity by pushing subgrid effects to the decoupled level of local equilibrium thermodynamics.

### 3. Decaying turbulence

In this section, we compare the results of the Entropic Lattice Boltzmann simulation with those of pseudo-spectral simulation of the Navier-Stokes equations (hereafter SS) for the case of two-dimensional, homogeneous, incompressible decaying turbulence. In this setup, one starts with a Gaussian random field in a periodic box, and probes the decay of the turbulent field.

The initial conditions are given by a zero-mean Gaussian vorticity field with random Fourier phases. The functional form of the energy spectrum is frequently chosen as:

$$E(k) = C_0 k^A [1 + (k/k_0)^{B+1}]^{-1}, \quad (3.1)$$

where,  $C_0$  is a normalization constant and parameters  $A$ ,  $B$  and  $k_0$  are chosen in such a way that the energy spectrum remains narrow banded (Bracco *et al.* 2000).

As a SS algorithm, we use the pseudo-spectral method, i.e., the non-linear terms are evaluated in real space, with a formulation in primitive variables (the two velocity com-

ponents). The equation to be solved in Fourier space looks as follows:

$$\frac{\partial \hat{u}_i}{\partial t} + jk_j \widehat{(u_j u_i)} = -jk_i \hat{p} + \frac{1}{Re} k^2 \hat{u}_i \quad (3.2)$$

where the symbol  $\hat{Q}$  denotes the Fourier transform of the quantity  $Q$ . At each time step the nonlinear term is projected onto a solenoidal field in order to maintain incompressibility condition  $k_i \hat{u}_i = 0$ ; this procedure is straightforward in  $k$ -space, being  $\mathcal{P}(jk_j \widehat{(u_j u_i)}) = jk_j (\delta_{il} + u_i u_l / k^2) \widehat{(u_j u_l)}$ , where  $\mathcal{P}$  is the projecting operator. The evaluation of the nonlinear terms is performed with a 3/2-dealiased pseudo-spectral method. For the time-marching, a semi-implicit low storage third-order accurate Runge-Kutta scheme was used (Spalart 1988).

In the following subsections, a detailed comparison of the result of decaying turbulence simulated with SS and ELBM is presented.

### 3.1. Fully-resolved simulation

We consider a two-dimensional box of length  $L = 512$  and viscosity  $\nu = 5.0 \times 10^{-4}$  (all quantities are in lattice units), for the SS as well as the ELBM. As described earlier, the initial conditions are given in Fourier space with  $k_0 = 0.2$ ,  $A = 6$  and  $B = 17$  (see Eq. 3.1). The initial spectrum is reasonably peaked at low wave numbers. The initial velocity profile has mean kinetic energy  $E(t = 0) = 1.64505947 \times 10^{-4}$  and the mean enstrophy is  $Z(t = 0) = 2.0348495 \times 10^{-6}$ . A rough estimate of the eddy turnover time is  $t_e \approx Z^{-1/2} \approx 700$  (Bracco *et al.* 2000). The Reynolds number based on the mean initial kinetic energy and the box-length as the characteristic length is  $Re = L\sqrt{(2E)}/\nu \approx 13134$ . The estimated dissipation length is  $L_d \sim L Re^{-1/2} \approx 3.2$ .

The agreement between the two simulations is very good up to  $t/t_e \sim 20$ . As, shown in figure 2, at  $t/t_e \sim 30$  (i.e.,  $t \sim 20000$ ) slight difference between the two methods starts to show up in the vorticity contour plot. However, this difference is only in the small scale features of the flow, while all large scales are still the same at this time.

Figure 3 shows a comparison of the energy and enstrophy spectra, respectively, up to  $t = 10000$ . The plot shows that the energy and the enstrophy are narrow banded initially. The enstrophy and the energy plots for the SS show the typical behavior, where during the course of simulation high wave number modes start gaining enstrophy (and consequently some energy too).

In freely decaying 2D turbulence, dissipation takes place via an enstrophy cascade from large to small scales. To prevent enstrophy pile-up, a small-scale enstrophy sink is typically required in numerical simulations. Figure 3 shows that the ELBM naturally provides a cutoff at high wave-number. In the subsequent section, we shall show that this cutoff does not affect the low wave-numbers region in any unphysical manner.

Figure 4 shows the energy and enstrophy time decay respectively. We see that these quantities are slightly underestimated by the ELBM. This is probably related to the sharp cutoff at high wavenumber present in the ELBM simulation.

As the simulation is performed in the low-Reynolds number regime, both methods provide a rather poor agreement with the Kolmogorov-Batchelor theory, and show visible deviations from the theoretically expected spectrum  $E(k) \sim k^{-3}$ .

### 3.2. Unresolved simulation: example I

In the previous section, 3.1, we have verified that the entropic method can be used to perform a fully resolved simulation of turbulence. We also observed that when the spectrum is not fully resolved by the computational domain, the ELBM method introduces a

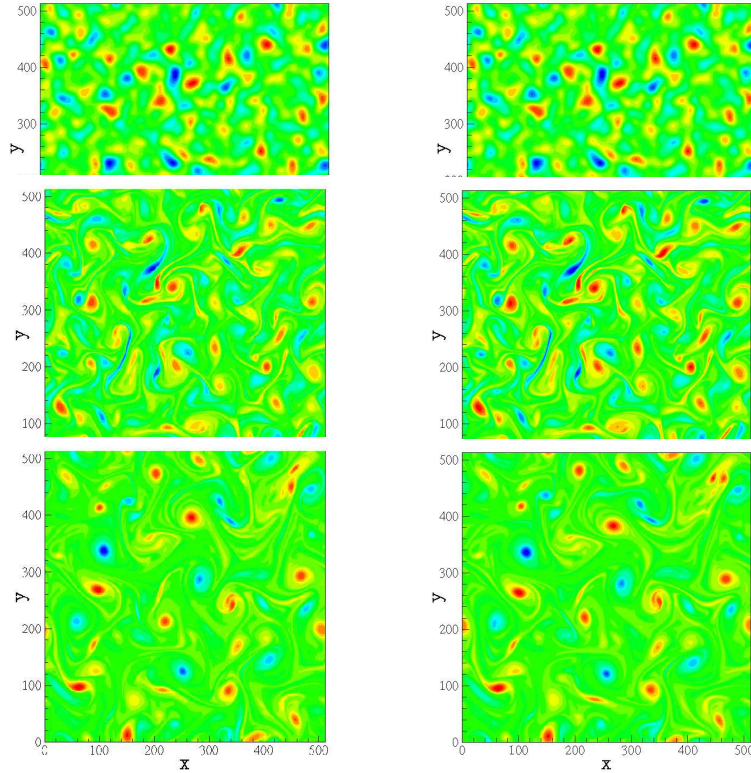


FIGURE 2. Contour plots of vorticity at  $t = 0, 5000, 20000$ : ELBM results (right column), spectral results (left column). Approximate eddy turnover time is  $t_e = 700$ .

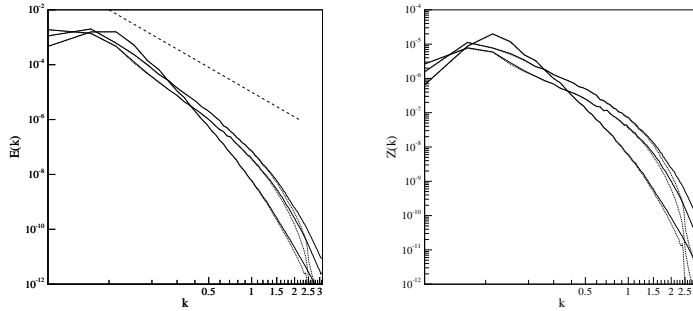


FIGURE 3. Energy and enstrophy spectra (left and right plot respectively) in the fully resolved simulation (example II) for three different times:  $t = 1000, 5000, 10000$ . Solid line is for spectral simulation and the dotted symbols represent ELB simulation. A dashed line showing  $k^{-3}$  spectra in the energy spectra is also shown.

sharp dissipation at high wave numbers. In this section, we shall explore how such high- $k$  cut-off affects the spectrum of the resolved scales.

In order to magnify this effect, for the spectral simulation we used  $256 \times 256$  grid points, while for the ELB we performed the simulation with  $128 \times 128$  grid points. We prepare the initial condition in such a way that the resolved scales are the same for both methods (see plot on the left hand side in figure 5). The spectral simulation is fully resolved while

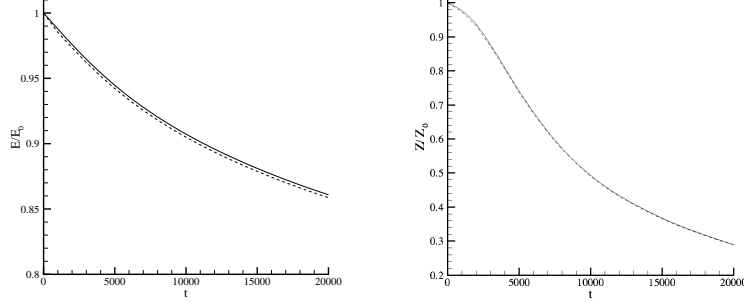


FIGURE 4. Time history of the energy (left plot), and the enstrophy.  $E_0$  and  $Z_0$  are the energy and the enstrophy respectively at  $t = 0$ . Solid line SS and dotted line ELBM.

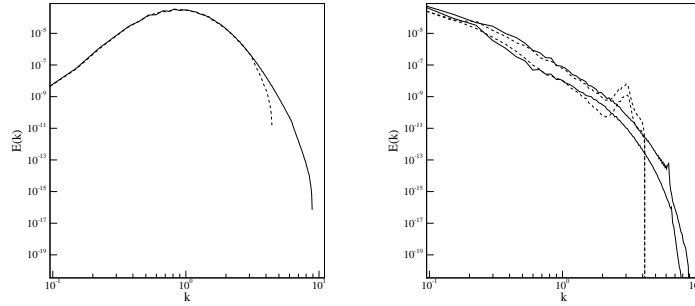


FIGURE 5. Wave number energy spectra in the unresolved simulation (example I). The plot on the left hand side shows the initial condition, while that on the right hand side shows the energy spectra for three different times:  $t = 4000$ ,  $20000$ ,  $40000$ . The solid line is for the spectral simulation and the dashed symbols represent ELB simulation

the spectrum for the ELBM simulation is truncated almost in the middle. The plot of the energy spectra, figure 5, at different times shows that the ELBM simulation follows the spectral simulation reasonably well. At low wave-numbers, i.e., in the resolved scales, the deviation from the spectral simulation is quite small. Near the cutoff wavenumber, a slight (but localized) hump in the profile obtained from ELBM appears. This hump and the agreement at low wavenumbers, can be interpreted as a signature of the very localized nature of the ELBM dissipative cut-off at high wavenumbers.

### 3.3. Unresolved simulation: example II

In the previous two sections, we showed that the entropic method can perform turbulence simulation, both resolved and underresolved, to a reasonable degree of accuracy. In this section, we shall explore the ELBM behaviour for flows much beyond the grid resolution. For this case, we have chosen the box-size as  $L = 512$  and viscosity  $\nu = 5.0 \times 10^{-6}$  for the ELBM simulation. As described earlier, the initial conditions are given in Fourier space with  $k_0 = 0.2$ ,  $A = 6$  and  $B = 17$  (see Eq. 3.1). The initial velocity profile has mean kinetic energy  $E(t = 0) = 1.20861512 \times 10^{-4}$  and mean enstrophy as  $Z(t = 0) = 1.4949915 \times 10^{-6}$ . A rough estimate of the eddy turnover time is  $t_e \approx Z^{-1/2} \approx 818$  (Bracco *et al.* 2000). The Reynolds number based on the mean initial kinetic energy and the box-length as the characteristic length is  $Re = L\sqrt{(2E)}/\nu \approx 1.59 \times 10^6$ . The



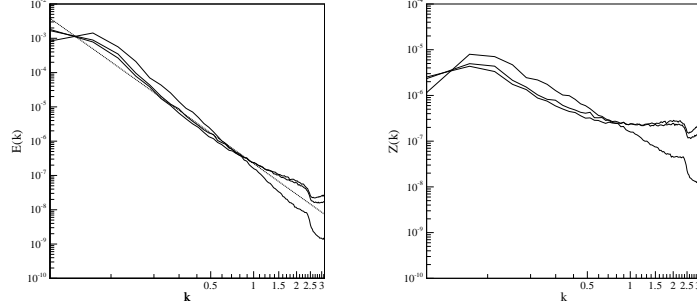


FIGURE 6. Energy and enstrophy spectra (left and right plot respectively) in the ELBM unresolved simulation (example II) for three different times:  $t = 5000, 15000, 20000$ . A dashed line showing  $k^{-3}$  spectra in the energy spectra is also shown.

dissipation length scale is estimated as  $L_d \sim L Re^{(-1/2)} \approx 0.4$ . Figure 6 shows that during the time evolution, Batchelor spectra  $E_k \sim k^{-3}$  for the energy and  $k^{-1}$  for the enstrophy in the inertial regime, are reproduced to a reasonable accuracy. The scaling law is best fitted at  $t = 15000$  as  $2 \times 10^{-7} k^{-3}$ . A rough estimate of the enstrophy transfer rate yields  $1.7 \times 10^{-11}$ . This gives a value of 4.8 for the constant appearing in the Batchelor scaling, while the theoretical value is 2.626. We remind that the determination of this constant requires an accurate evaluation of the enstrophy transfer rate, so that we expect the agreement to improve with increasing system size. The agreement with the scaling law in such an underresolved simulation shows that the ELBM exhibits a sort of built-in subgrid model for turbulent flows.

It is argued that in two-dimensional isotropic turbulence, the eddy-viscosity develops a dependence on the wavenumber and may depart from its mean value in both positive and negative directions (Kraichnan 1976). It is therefore of interest to investigate whether ELBM has similar features. We can argue that the deviation of the effective relaxation frequency  $\alpha\beta$  from its near equilibrium value  $2\beta$  is related to the deviation of viscosity from the molecular viscosity  $\nu(\beta) = c_s^2(1/2\beta - 1/2)$ . In order to parameterise the relaxation behavior, we define the ‘effective viscosity’ of the ELBM fluid (in lattice units) as:

$$\nu_{\text{eff}} = c_s^2 \left( \frac{1}{\alpha\beta} - \frac{1}{2} \right). \quad (3.3)$$

In figure 7 the probability distribution of turbulent fluctuations in effective viscosity as compared to the bare molecular viscosity,  $\delta\nu/\nu = \nu_{\text{eff}}(\alpha, \beta)/\nu(\beta) - 1$  is plotted. From this figure a three-modal distribution is clearly visible, corresponding to three distinct classes of events:

- 1) Plus-events, ( $\delta\nu/\nu > 0$ ): Effective viscosity is much larger than molecular viscosity.
- 2) Normal-events, ( $\delta\nu/\nu = 0$ ): Effective viscosity is identical to molecular viscosity, within the machine accuracy.
- 3) Minus-events, ( $\delta\nu/\nu < 0$ ): Effective viscosity is much smaller than molecular viscosity. This case corresponds to local micro-instability.

The relative weights,  $\{M_{\text{Plus}}, M_{\text{Normal}}, M_{\text{Minus}}\}$ , for the three events at three different times,  $t = 1000, 5000, 10000$ , are  $\{0.227002, 0.754618, 0.018380\}$ ,  $\{0.099759, 0.853831, 0.046590\}$ , and  $\{0.097823, 0.839673, 0.062504\}$ , respectively. This shows that, the number of Minus-events grows in time, while Plus-events do the opposite. The above figures have been obtained by defining Normal-events via the condition  $|\delta\nu/\nu| < 0.01$ . Such a low threshold indicates that the distribution of Normal-events is a Dirac’s delta. This shows that

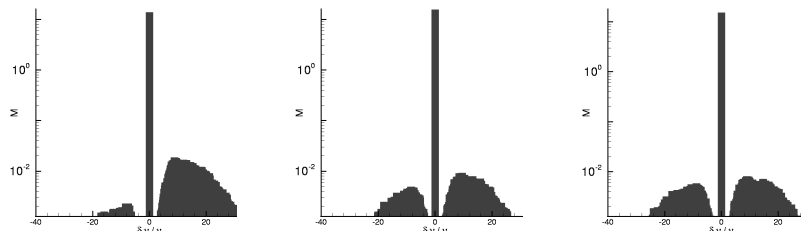


FIGURE 7. Distribution  $M$  of  $\delta\nu/\nu$  at time  $t = 1000, 5000, 10000$  in a unresolved simulation. Notice the delta function at  $\delta\nu/\nu = 0$ , where the distribution is normalised in such a way that area under curve is unity.

the parameter  $\alpha$  is highly ‘intermittent’, e.g. quiescent in most part of the flow, with strong bursts of activity in small regions (this is confirmed by visual inspection of the spatial distribution  $\alpha(x, y)$ , not shown here). This type of behaviour cannot be captured by any ‘conventional’ picture of eddy-viscosity.

#### 4. Conclusions

In conclusion, we have shown that entropic lattice Boltzmann models (ELBM) can cope with the instabilities which plague standard lattice Boltzmann schemes in a regime where subgrid scales are dynamically excited. This boost of numerical stability is the result of securing compliance with the H-theorem, hence positivity of the discrete distribution function. Therefore it can be concluded that ELBM exhibit a built-in subgrid model which is rooted in a basic principle of statistical mechanics rather than on heuristic requirements or high-order discretizations of the Navier-Stokes equations. This built-in model cannot be reduced to an algebraic relation between eddy-viscosity and the large scale shear. This is not surprising, since the present ELBM accounts for both positive and negative turbulent relaxation, the latter corresponding to local instabilities which escape traditional eddy-viscosity turbulence models. Future work will tell whether such encouraging qualitative features can be turned into a quantitative *genuinely kinetic* approach to the problem of turbulence modeling.

#### REFERENCES

- Ansumali, S. and Karlin, I. V. (2002a). Entropy function approach to the lattice Boltzmann method. *J. Stat. Phys.*, **107**, 291–308.
- Ansumali, S. and Karlin, I. V. (2002b). Single relaxation time model for entropic lattice Boltzmann methods. *Phys. Rev. E*, **65**, 056312.
- Ansumali, S. and Karlin, I. V. (2002c). Minimal entropic kinetic models for simulating hydrodynamics. *cond-mat/0205510*.
- Benzi, R. and Succi, S. (1990). Two dimensional turbulence with the lattice Boltzmann equation. *J. Phys. A*, **23**(1), L1–L5.
- Benzi, R., Succi, S., and Vergassola, M. (1992). The lattice Boltzmann equation- theory and applications. *Phys. Rep.*, **222**, 145.
- Boghossian, B. M., Yepetz, J., Coveney, P. V., and Wagner, A. J. (2001). Entropic lattice Boltzmann methods. *Proc. Roy. Soc. Lond. A*, **457**, 717.

- Bracco, A., McWilliams, J. C., Murante, G., Provenzale, A., and Weiss, J. B. (2000). Revisiting freely decaying two-dimensional turbulence at millennial resolution. *Phys. Fluids*, **12**, 2931–2941.
- Chen, H., Succi, S., and Orszag, S. (1999). Analysis of subgrid scale turbulence using the Boltzmann Bhatnagar–Gross–Krook kinetic equation. *Phys. Rev. E*, **59**, R2527.
- Chen, H., Kandasamy, S., Orszag, S., Shock, R., Succi, S., and Yakhot, V. (2003). Extended-Boltzmann kinetic equation for turbulent flows. *submitted to Science*.
- Karlin, I. V., Ferrante, A., and Öttinger, H. C. (1999). Perfect entropy functions of the lattice Boltzmann method. *Europhys. Lett.*, **47**, 182–188.
- Kraichnan, R. H. (1976). Eddy viscosity in two and three dimension. *J. Atmos. Sc.*, **33**, 1522.
- Lesieur, M. and Metais, O. (1996). New trends in large-eddy simulations of turbulence. *Ann. Rev. Fluid Mech.*, **28**, 45–82.
- Martinez, D. O., Matthaeus, W. H., Chen, S., and Montgomery, D. C. (1994). Comparison of spectral method and lattice Boltzmann simulations of two-dimensional hydrodynamics. *Phys. Fluids*, **6(3)**, 1285–1298.
- Shan, X. and He, X. (1998). Discretization of the velocity space in the solution of the Boltzmann equation. *Phys. Rev. Lett.*, **80**, 65.
- Spalart, P. R. (1988). Direct simulation of a turbulent boundary layer up to  $R = 1410$ . *J. Fluid Mech.*, **187**, 61.
- Succi, S. (2001). *The Lattice Boltzmann Equation for Fluid Dynamics and Beyond*. Oxford University Press, Oxford.
- Succi, S., Karlin, I. V., and Chen, H. (2002). Role of the  $H$  theorem in lattice Boltzmann hydrodynamics. *Rev. Mod. Phys.*, **74**, 1203–1220.